Research Square

Preprints are preliminary reports that have not undergone peer review.
They should not be considered conclusive, used to inform clinical practice,
or referenced by the media as validated information.

Thermal, wetting and microstructural properties of the tin (Sn)-58%bismuth (Bi) solder joint at 160 °C, 170°C and 180 °C

Tee Boon Hean
Taylor's University
Amares Singh
amares.singh@taylors.edu.my

Taylor's University
Tan Wei Hong
Universiti Malaysia Perlis (UniMAP)
Choo Hui Leng
Taylor's University
Muhammad Amir Aziat Ishak
The National University of Malaysia
Bahman Nasiri -Tabrizi
Taylor's University
Rubentheren Viyapuri
Universiti Tunku Abdul Rahman
Ervina Efzan Mhd Noor
Multimedia University

Research Article

Keywords: SnBi solder joint, thermal properties, wettability, intermetallic compound

Posted Date: July 1st, 2026

DOI: https://doi.org/10.21203/rs.3.rs-10130492/v1

License: This work is licensed under a Creative Commons Attribution 4.0 International License.
Read Full License

Additional Declarations: No competing interests reported.

Version of Record: A version of this preprint was published at Journal of Materials Science: Materials in Electronics on September 15th, 2026. See the published version at https://doi.org/10.1007/s10854-026-18461-9.

Thermal, wetting and microstructural properties of the tin (Sn)-58%bismuth (Bi) solder joint at 160 °C, 170°C and 180 °C

Tee Boon Hean[1], Amares Singh[1*], Tan Wei Hong[2], Choo Hui Leng[1], Muhammad Amir Aziat Ishak[3], Bahman Nasiri-Tabrizi[1], Rubentheren Viyapuri[4], Ervina Efzan Mhd Noor[5]

[1] School of Engineering, Faculty of Innovation & Technology, Taylor's, University, 47500 Subang Jaya, Selangor, M alaysia

[2] Faculty of Mechanical Engineering & Technology, Universiti Malaysia Perlis (UniMAP), Pauh Putra Campus, 02600 Arau, Perlis, Malaysia.

[3] Solar Energy Research Institute (SERI) The National University of Malaysia, 43600 Bangi, Selangor, Malaysia.

[4] Lee Kong Chian Faculty of Engineering and Science, Universiti Tunku Abdul Rahman, Jalan Sungai Long, Bandar Sungai Long,
43000 Kajang, Selangor, Malaysia.

[5] Faculty of Engineering and Technology, Multimedia University, Jalan Ayer Keroh Lama,
75450, Bukit Beruang, Melakaa.

[*] Corresponding author: amares.singh@taylors.edu.my

Abstract.
The thermal, wetting and microstructural properties of tin (Sn)-58% bismuth (Bi) solder joints were investigated at three reflow temperatures of 160, 170, and 180 °C to assess their performance for low-temperature assembly processes. Differential scanning calorimetry (DSC) analysis revealed that the SnBi alloy exhibited a melting range between 139 and 145 °C, confirming its low temperature applicability for reduced thermal processing conditions. Contact angles were measured at 78.4°, 68.95°, and 69.39° at 160, 170 and 180 °C, respectively, classifying the SnBi as having moderate wettability behavior. The spreading ratios of 347.7, 333.7 and 322.8 for 160, 170 and 180 °C was measured demonstrating an inverse relationship with contact angle in accordance with wetting theory. The microstructural observations from scanning electron microscopy image (SEM) at the SnBi/Cu solder joint revealed the formation of a relatively uniform Cu_6Sn_5 intermetallic compound (IMC) layer at 170 and 180 °C, whereas minimal or nearly no IMC formation was observed at 160 °C due to insufficient interfacial reaction. The findings indicate that SnBi solder joint at the lower reflow temperature of 160, 170, and 180 °C showed acceptable wettability condition and interfacial characteristics, supporting its potential application for energy-efficient and thermally sensitive microelectronic assembly processes.

Keywords: SnBi solder joint, thermal properties, wettability, intermetallic compound

1.0 Introduction

Soldering is a metallurgical joining process in which two or more metallic materials are interconnected using a filler metal, commonly referred to as solder, at temperatures below 450 °C [1]. For several decades, eutectic tin–lead (SnPb) solder has remained the dominant interconnection material in electronic packaging owing to its excellent wettability, low melting temperature, and reliable mechanical performance. However, the toxicity of lead has raised significant environmental and human health concerns, leading to increasingly stringent international regulations restricting the use of lead-containing solders in electronic manufacturing industries [1,2]. Consequently, extensive research efforts have focused on the development and characterization of lead-free solder alloys with comparable or superior performance characteristics [2–4]. Among the various alternatives, tin–bismuth (SnBi) solder has emerged as a promising candidate due to its relatively low melting point of approximately 138 °C, high yield strength ranging from 25 to 35 MPa, cost-effectiveness, and favorable reliability performance [5]. In addition to these advantages, the thermal properties of SnBi solder further enhance their suitability for low-temperature electronic assembly applications.

Heat capacity is defined as the amount of heat energy required to raise the temperature of a body by one degree Celsius (°C) or one Kelvin (K). It represents the ability of a material or system to store thermal energy. The heat capacity, (C), is expressed as in Eq. (1).

$$C = \frac{Q}{\Delta T} \tag{1}$$

where (C) is the heat capacity (J/K), (Q) is the heat transferred to the system (J), and (Δ T) is the temperature change (K or °C). The heat capacity of SnBi alloy, as summarized in Table 1, ranges from approximately 1.0 to 3.0 J/mol·K near the eutectic composition, indicating relatively low thermal energy requirements during processing. A lower heat capacity is beneficial in soldering operations because it enables faster heating and cooling responses while reducing overall energy consumption during reflow. As presented in Table 1, the heat capacity (Cp) decreases from 2.93518

J/mol·K at 293 K to 1.04822 J/mol·K at 463.12 K. It is suggesting that progressively lower thermal energy is required to increase the alloy temperature at elevated thermal conditions.

The incorporation of Bi into the Sn matrix alters the thermal energy storage behavior of the alloy and contributes to the reduction in heat capacity with increasing temperature. This behavior is strongly influenced by the presence of bismuth, which possesses distinct atomic vibrational and thermal characteristics compared to tin. Furthermore, the eutectic interaction between Sn and Bi lowers the overall melting temperature of the alloy, thereby enabling phase transformation at reduced thermal input. The synergistic interaction between Sn and Bi therefore enables SnBi solder alloys to exhibit enhanced thermal efficiency, reduced processing energy requirements, and favorable characteristics for low-temperature microelectronic interconnection applications.

Table 1. Thermal energy at different temperature for Sn52Bi

Temperature (K)	Heat Capacity, C_p (J/mol·K)
293	2.93518
298	2.88646
415.5	1.60947
463.12	1.04822

Solidus and liquidus temperature are critical thermal properties that determine the solidification range [4,7]. The temperature interval between these two points, commonly referred to as the solidification range, plays a significant role in determining the resulting microstructure and overall joint integrity. A lower solidification range is desired as it produces well-defined and compact microstructure and reduces micropores defects [7]. Table 2 summarizes selected literature pertaining to the solidification interval, solidus and liquidus temperature of some SnBi compositions. Many researchers study on the eutectic Sn58Bi composition [11,12,13] exhibits the lowest melting characteristics, with a relatively narrow solidification interval ranging from approximately 3 to 9 °C compared others alloy. As content of Bi decreases, the solidification interval and liquidus temperature increases, meaning the transition from solid to liquid state will take place over a longer period.

Table 2. Thermal properties of different compositions of SnBi.

Solder Composition	Solidus (°C)	Liquidus (°C)	Solidification Interval (°C)	References
Sn58Bi	130.2	139	8.8	[6]
	136.1	139.1	3	[8] [9]
	139	143.1	4.1	[10]
	139.3	147.6	8.3	[11]
	139.5	147.6	8.1	[12]
	139.4	148	8.6	[13]
	139.6	147.4	7.8	[14]
	140.3	146	5.7	
Sn55Bi	138	144	6	[15]
Sn50Bi	138	155	17	
Sn45Bi	138	168	30	
Sn40Bi	138	178	40	
Sn35Bi	138	186	48	

Wettability properties involving the wetting angle and spreading ratio are used to assess the quality of a solder joint. Low contact angles in reactive wetting are often used as an indicator for strong solder connections [16]. Griffiths et al. [16] performed an investigation on the wetting angle of SnBi solder based on different compositions at 350 and 500°C and noticed decrease in the wetting angle until the eutectic composition is reached which later increases as the Bi content increases. In that study, a minimum wetting angle is observed for both temperatures between 20 and 30 at. %-Bi. The increase in temperature will result in a decrease in wetting angle. The result aligns with He et al. [17], where the investigation revealed the contact angle for eutectic SnBi with flux was 45.22° at 200°C [18,19]. It appears that the composition as well as temperature of SnBi influences the quality of solder joint, yet detailed investigation at a specific reflow temperature is not really investigated.

Furthermore, investigations on SnBi solder under reflow conditions provided essential insight into the microstructural evolution and interfacial metallurgical reactions governing solder joint formation. Jayesh and Elias [20] reported that at elevated reflow temperatures of approximately 185°C, porous Cu_3Sn IMC formation is observed, whereas such porosity is absent at 170°C, indicating that reflow temperature plays a decisive role in controlling IMC morphology. These findings clearly demonstrate that thermal processing conditions significantly influence the formation mechanism and stability of interfacial IMCs in SnBi/Cu solder systems. Similarly, Zou et al. [21] conducted a comprehensive study on SnBi/Cu solder joints over a wide reflow temperature range between 180 to 300 °C. The investigation revealed that increasing reflow temperature promotes pronounced Bi segregation, which substantially alters microstructural homogeneity and interfacial reaction behavior. Although SnBi-based solder systems have been extensively explored, the fundamental understanding of SnBi/Cu solder joint behavior particularly with respect to the coupled effects of reflow temperature on thermal response, wettability, microstructural evolution and interfacial metallurgical reactions, remains insufficiently established. This gap is significant, as these parameters directly govern joint reliability and long-term performance in electronic packaging applications. Accordingly, this study aims to investigate the thermal characteristics, wettability parameter, microstructural properties and interfacial intermetallic formation of SnBi/Cu solder joints under controlled low reflow temperature conditions.

2.0 Materials and Methods

The Sn58%Bi solder alloy was prepared using high-purity raw materials of 99.99 wt.% tin (Sn) ingots and 99.99 wt.% bismuth (Bi) pieces. The elements were accurately weighed according to the eutectic composition of 42 wt.% Sn and 58 wt.% Bi to achieve the lowest melting temperature according to the phase diagram. The weighed elements were subsequently homogenized and melted in a furnace at 600°C for 1h to ensure complete alloying and compositional uniformity. The resulting Sn58Bi alloy was subjected to differential scanning calorimetry (DSC) and thermogravimetric analysis (TGA) to evaluate its thermal characteristics and melting behavior. Following solidification, the SnBi solder alloy was cast into billets for subsequent experimental characterization. These billets were then reflow-soldered onto copper (Cu) substrates at three different temperatures, namely 160, 170, and 180°C, with a fixed dwell time of 60s. The soldering process was carried out using a controlled hotplate system and a thermocouple was employed to ensure accurate and stable temperature conditions throughout the reflow process. After soldering, the samples were sectioned for analysis, and the contact angle and spreading ratio were measured for each reflow condition. Fig. 1 shows the cross-section samples used for the contact angle measurement. The spreading ratio was calculated using Eq. (2).

$$\text{Spreading Ratio} = \left(\frac{D-H}{D}\right) \times 100\% \tag{2}$$

where D is the diameter of the spread, and H is the height of the solder.

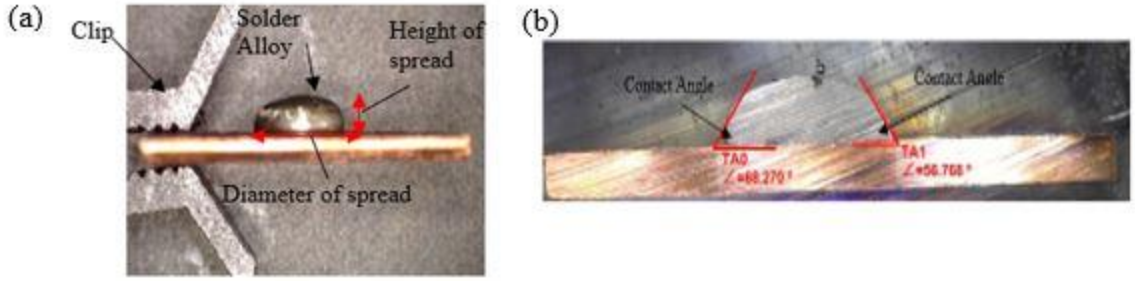

Fig.1 Wetting samples for (a) spreading ratio and (b) contact angle.

To examine the microstructural and metallurgical characteristics of the Sn58Bi/Cu solder joints, scanning electron microscopy (SEM) was employed to inspect the interfacial morphology and overall microstructural evolution with high spatial resolution. The SEM incorporated with energy-dispersive X-ray (EDX) was utilized to determine the elemental distribution and compositional variations across the solder/substrate interface. Furthermore, X-ray diffraction (XRD) analysis was conducted to detect the IMC formation and phase evolution at the SnBi solder joint for the different reflow temperatures.

3.0 Results and Discussion

3.1 DSC and TGA

The thermal analysis via the DSC peak in Fig. 2 revealed a melting peak at approximately 141°C, which is in close agreement with previously reported melting temperatures of eutectic SnBi alloys, typically ranging from 138 to 141°C [20 - 22]. The close agreement between the measured and reported values confirms the successful preparation of the eutectic SnBi composition and demonstrates the reliability of the fabrication procedure employed in this study. The slight elevation in melting temperature relative to the nominal eutectic value of 138 °C may be attributed to minor compositional deviations introduced during the weighing and mixing of the constituent elements. Previous investigations have demonstrated that even small variations in the Sn-to-Bi ratio can influence the melting characteristics and phase transformation behavior of SnBi-based alloys due to changes in microstructural homogeneity and phase distribution [21,22]. Such deviations are commonly observed in experimentally fabricated solder alloys and generally remain within the acceptable range for eutectic systems. The measured melting temperature of 141°C therefore remains representative of a eutectic SnBi alloy and is comparable to values reported in the literature [20–22]. The narrow melting interval indicates a relatively homogeneous microstructure and confirms the near-eutectic nature of the alloy. A narrow melting range is highly desirable for soldering applications because it promotes rapid melting and solidification, reduces thermal gradients during reflow processing, and minimizes the thermal stress imposed on electronic components and substrates [23].

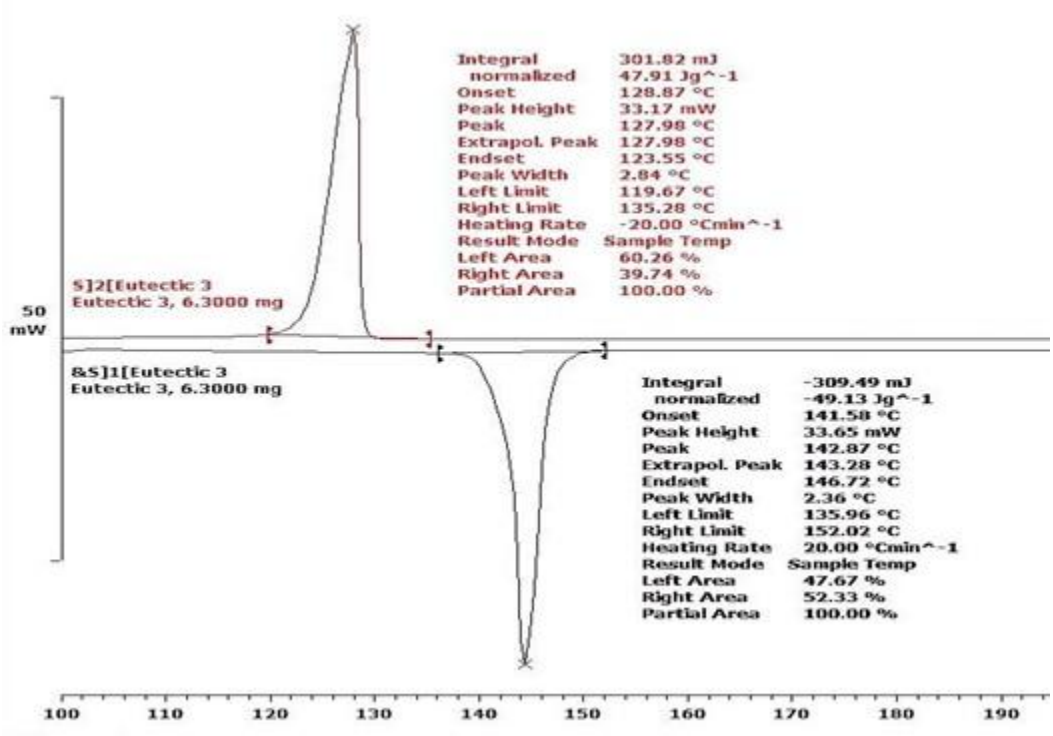

Fig.2 DSC curve of SnBi.

The TGA curve of the SnBi alloy is presented in Fig. 3. The TGA results indicate that the sample experienced a gradual mass reduction throughout the heating cycle under an oxygenated atmosphere. The initial sample mass of 2.825194mg decreased to 2.683968mg after heating at a rate of 10°C min^{-1}, corresponding to a total mass loss of 0.141226 mg. The percentage weight loss was determined using Eq (2), yielding a value of approximately 4.99wt.%. The observed reduction in mass suggests the occurrence of thermally activated physicochemical processes during heating. In oxygen-containing environments, such behavior is commonly attributed to the removal of physically adsorbed moisture, volatilization of residual organic contaminants, decomposition of surface impurities, and oxidation-induced reactions occurring at elevated temperatures [24–27]. The initial stage of weight reduction observed below approximately 150°C is likely associated with the evaporation of moisture and desorption of weakly bonded surface constituents. As the temperature increases, the rate of mass loss becomes more pronounced, indicating the activation of additional thermal

degradation mechanisms and oxidation-related processes. The overall weight loss percentage was calculated as in Eq (3).

$$\frac{2.683968-2.825194}{2.825194} \times 100\ \% = -4.99881\% \quad (3)$$

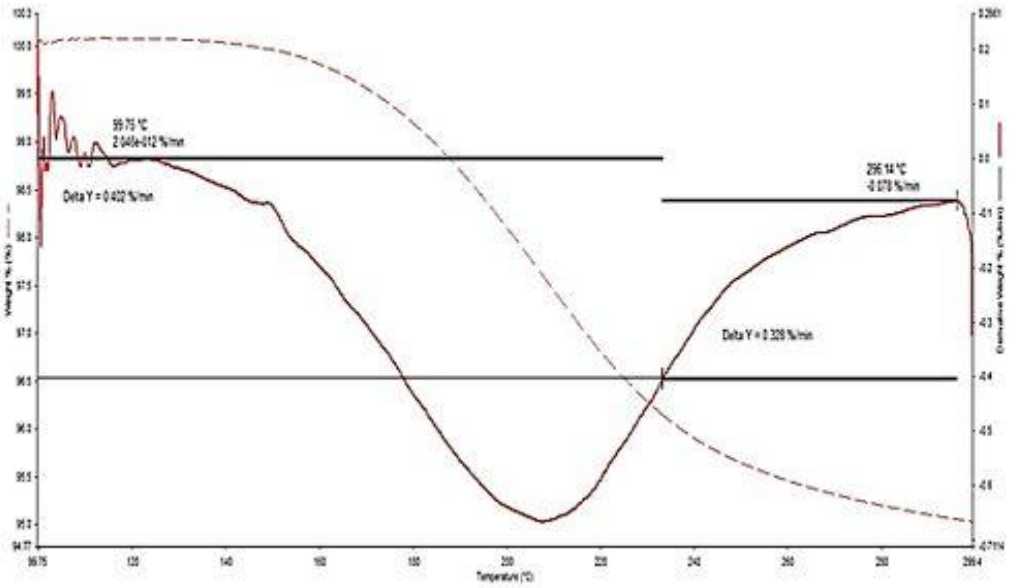

Fig.3 TGA curve of SnBi.

A closer examination of the TGA profile reveals that the onset of measurable mass reduction occurs at approximately 138°C which corresponds closely to the melting temperature identified from the DSC analysis. This agreement suggests that the thermal events observed in both analyses are associated with the eutectic phase transformation of the alloy. The initiation of melting enhances atomic mobility and increases surface activity, thereby facilitating the release of volatile species adsorbed on the alloy surface. The close correlation between the DSC and TGA results therefore confirms the thermal consistency of the fabricated eutectic SnBi alloy. The mass-loss rate becomes increasingly pronounced between approximately 170 and 230 °C, indicating that the dominant degradation processes occur within this temperature interval. As shown, the maximum mass-loss rate was observed at approximately 206 to 210°C, reaching about 0.402 % min^{-1}. This temperature region corresponds to the steepest section of the TGA curve and signifies the highest rate of volatile species evolution. Beyond 230°C, the DTG signal gradually approaches zero, indicating a substantial reduction in reaction kinetics and suggesting that most volatile constituents have already been removed. The damping behavior observed at higher temperatures further indicates that the alloy approaches a thermally stable condition after the completion of the primary degradation processes.

Importantly, the overall mass reduction remained below 5 wt.%, demonstrating that the alloy exhibits good thermal stability within the investigated temperature range. Considering that industrial reflow soldering processes for eutectic SnBi alloys are typically completed within a few minutes, the relatively slow mass-loss kinetics observed during TGA suggest that thermal degradation is unlikely to significantly influence solder performance under normal processing conditions. Consequently, the fabricated SnBi alloy exhibits thermal characteristics suitable for low-temperature electronic packaging applications, where thermal stability and process reliability are critical requirements.

3.2 Wetting Properties

The wettability of a solder alloy is commonly evaluated by its contact angle and spreading area. In general, lower contact angles indicate better wettability because the molten solder would spread more smoothly across the substrate surface. According to Young's equation, wettability improves when the interfacial energy between the solder and substrate decreases, allowing the solder to form a flatter droplet shape. Although the interfacial energy is not studied in this paper, the contact angle and spreading ratio was used to relate to the prior parameter. The chart as in Figs. 4 and 5 show the result of contact angles and spreading ratios at each reflow temperature. Among the three reflow temperatures, the solder joint at 160°C displayed the highest contact angle at 78.4°, followed by 69.39° at 180°C and 68.95° at 170°C, showing minimal variation. These contact angles are considered high and are attributed due to the

high Bi content present in the alloy as well as the associated surface tension. Bi are known to restrict the fluidity of the SnBi solders. Study by Griffiths et al. [16] too supported this observation, as the investigation revealed an increase in contact angle with the increase in Bi content, with the lowest contact angle at 20 wt.% to 30 wt.% of Bi content.

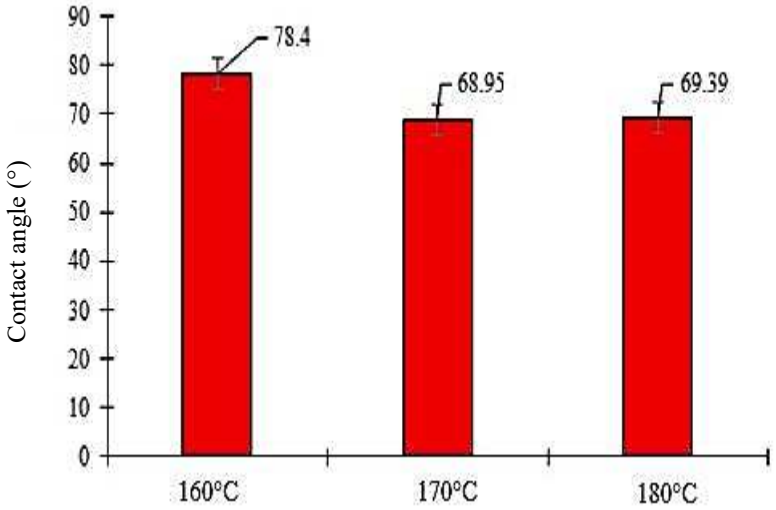

Fig. 4 Average contact angle of SnBi at 160°C, 170°C and 180°C.

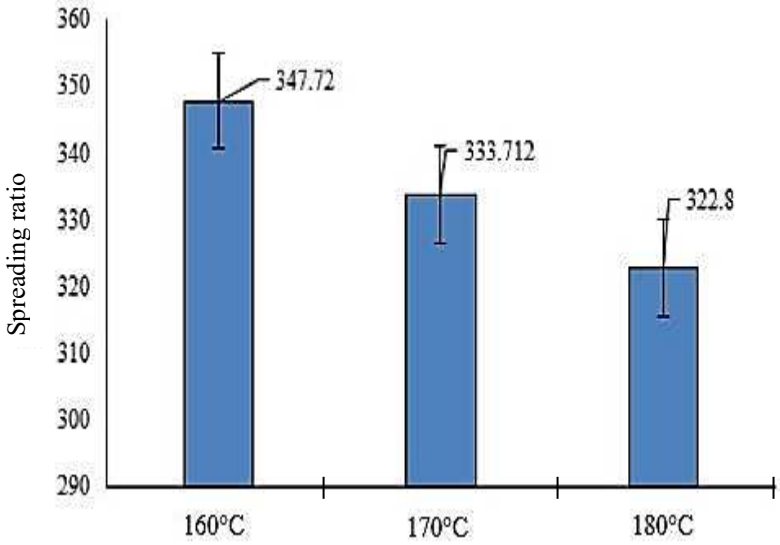

Fig. 5 Average spreading ratio of SnBi at 160°C, 170°C and 180°C.

The increase in temperature causes the reduction in the contact angle due to overheating, which increases the fluidity and spreading of alloy [24]. At higher temperatures, the viscosity of the molten solder decreases, enabling better flow and improved interaction with the substrate surface. Furthermore, elevated temperatures promote atomic diffusion at the solder–substrate interface, which enhances metallurgical bonding and reduces interfacial tension. These factors contribute to the improved wetting behaviour observed at 170°C**.** However, when the temperature further increased to 180°C**,** the contact angle increased slightly to 69.39°**.** This behaviour may be attributed to the formation of oxide films on the molten solder surface and substrate. Excessive heating can accelerate oxidation, which acts as a barrier between the solder and substrate, thereby limiting wetting performance. Additionally, prolonged exposure to higher temperatures may increase flux consumption, reducing its ability to remove oxides effectively. Consequently, the wettability improvement observed at 170°C was not further enhanced at 180°C.

There was a gradual decrease in spreading ratio from 347.72 to 322.80 with increasing temperature appears contrary to the expectation that better wettability should result in larger spreading areas. This phenomenon may be associated with changes in molten solder dynamics and IMC formation. At elevated temperatures, accelerated diffusion between the solder and substrate can promote the growth of IMC layers. Excessive IMC growth may restrict lateral spreading of the molten solder and alter its wetting kinetics. Moreover, increased oxidation at higher temperatures can hinder the outward flow of solder, resulting in a smaller spreading area despite the lower contact angle. The discrepancy between contact angle and spreading area suggests that wettability is influenced by multiple factors rather than a single parameter. While the contact angle indicates the thermodynamic tendency of the solder to wet the substrate, the spreading area reflects the actual flow behaviour of the molten solder during reflow. Therefore, both parameters should be considered simultaneously when evaluating solder performance.
The results indicate that 170°C is the optimum soldering temperature for the investigated solder alloy, as it produced the lowest contact angle and thus the best wetting performance. Temperatures above this optimum may promote oxidation and excessive interfacial reactions, which can adversely affect the spreading characteristics of the molten solder. These findings are consistent with previous studies reporting that an optimum soldering temperature exists where improved fluidity and interfacial bonding are achieved without significant oxidation or excessive IMC growth.

3.3 Microstructural and Metallurgical Properties

Microstructural and metallurgical properties of a solder are primarily influenced by the IMC formation and its thickness that influences a solder joint's reliability. The SEM analysis revealed that minimal IMCs were formed between the Sn58Bi solder and Cu substrate. Fig. 6 (a) displays the overall SEM image of the SnBi/Cu substrate. The EDX analysis on the SEM image of the Sn58Bi revealed minimal presence of Sn, Bi and Cu, with large void visible. The minimal presence of these elements clarified that the formation of voids is due to the trapped gas within the molten solder. This is because of the flux decomposition when heated throughout the soldering process and the gas will be released. The EDX point was taken at the area which appears to be void, as seen in Fig. 6 (b). Nevertheless, the void was seen at 160 °C, and the reason behind this is due to the incomplete outgassing occurrence as there is insufficient heat to fully activate the flux, resulting in trapped gas within the solidified solder.

(a)

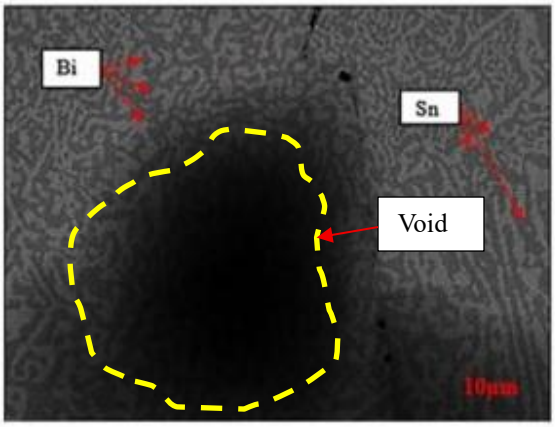

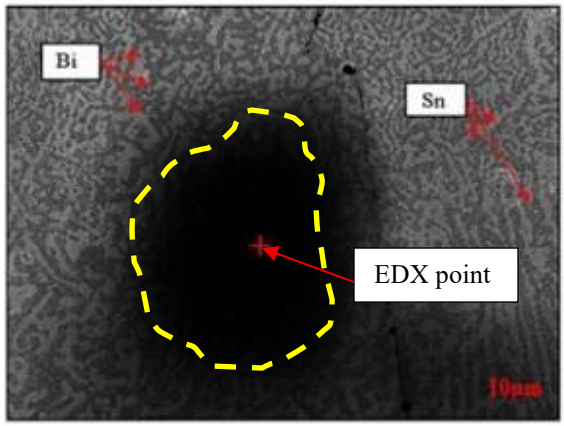

Sn58Bi's IMC formation rates are known to rapidly accelerate before slowing down over time [25]. According to the phase diagram of SnBi alloy, at temperature above 138°C, a rapid formation of IMC should begin but this may not be unanimous. Yu, J. and Kim J. Y. [26] observed that void formation at the interface disrupts the IMC growth rate [26]. In this study, the Sn, Bi and Cu elements did not react and produce IMCs due to insufficient heat as the reflow temperature is only 20°C (for 160 °C reflow temperature) higher than the melting point of SnBi. Even though the SnBi solder has melted, insufficient heat energy disables IMC layer formation. Another observation that proves that IMCs are not formed at 160°C is the presence of voids, as voids are known to be the gaps left from insufficient IMC formation. This was seen just above the solder joint, as in Fig. 6. Studies have proved that diffusion gaps left between the substrate and solder will result in the formation of voids [27, 28].
The SEM images of the SnBi/Cu solder joints at 170 and 180 °C are shown in Fig. 7 (a) and (b) respectively. The IMC layer thickness was measured using these cross sections and is shown in Fig. 8. The IMC layers of Cu_6Sn_5 and Cu_3Sn are detected from the EDX analyses and seen in Fig. 9 (a) and Fig. 9 (b). These IMCs were formed during the soldering process as the reaction between the Cu substrate and SnBi solder as in Eq (4). With the increase in soldering

temperature, Cu atoms are gradually consumed to support the growth of Cu_3Sn intermetallic compounds, as described in Eq (5). Subsequently, Cu_6Sn_5 begins to convert into Cu_3Sn, as illustrated in Eq (6).

$$6Cu + 5Sn \rightarrow Cu_6Sn_5 \quad (4)$$

$$Cu + 3Sn \rightarrow Cu_3Sn \quad (5)$$

$$Cu_6Sn_5 + 9Cu \rightarrow 5Cu_3Sn \quad (6)$$

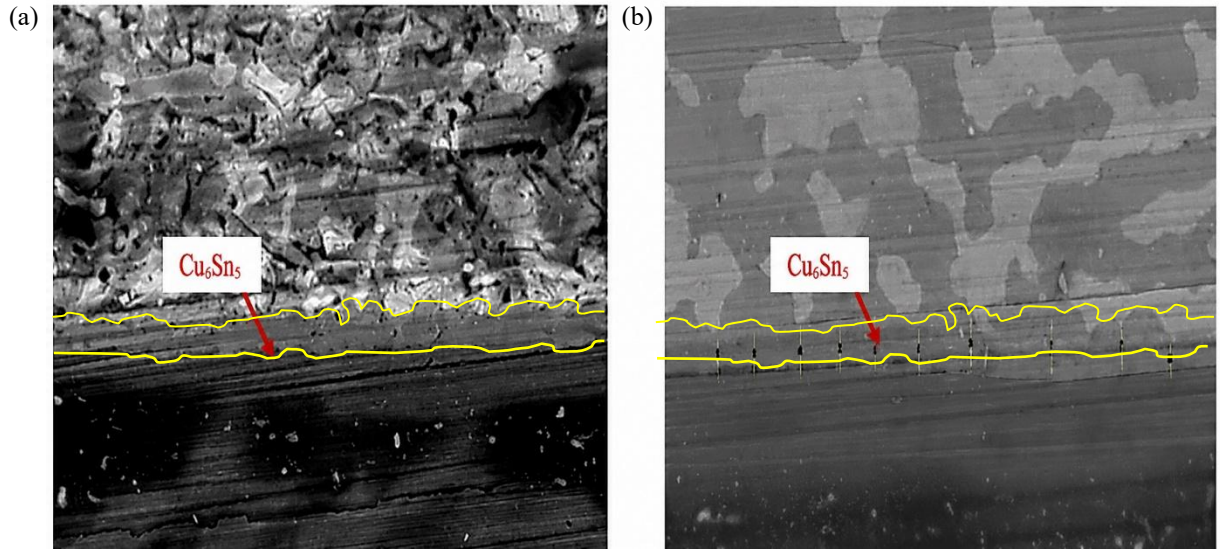

Fig. 7 (a) SEM images of the SnBi/Cu solder joints with the presence of Cu_6Sn_5 IMC at (a) 170 and (b) 180 °C

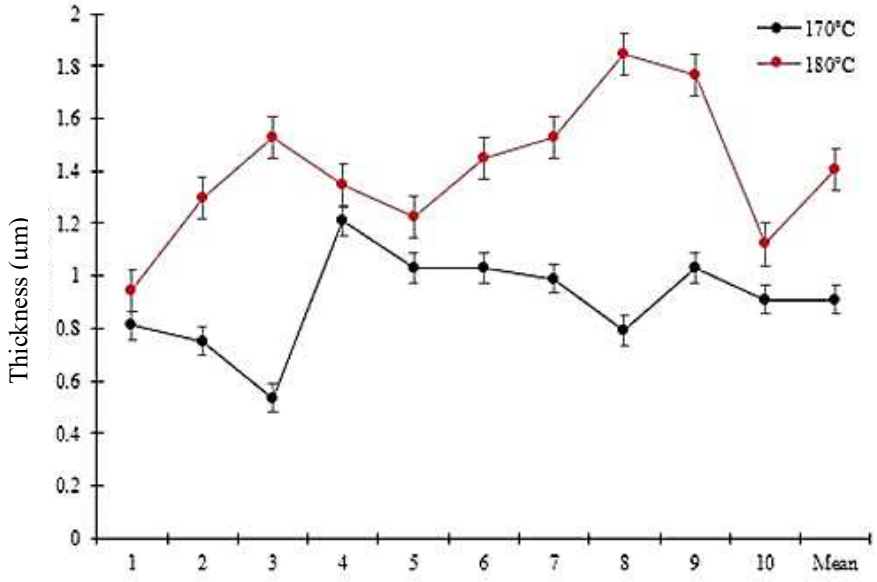

Fig. 8 Average Cu_6Sn_5 IMC layer thickness at 170°C and 180°C.

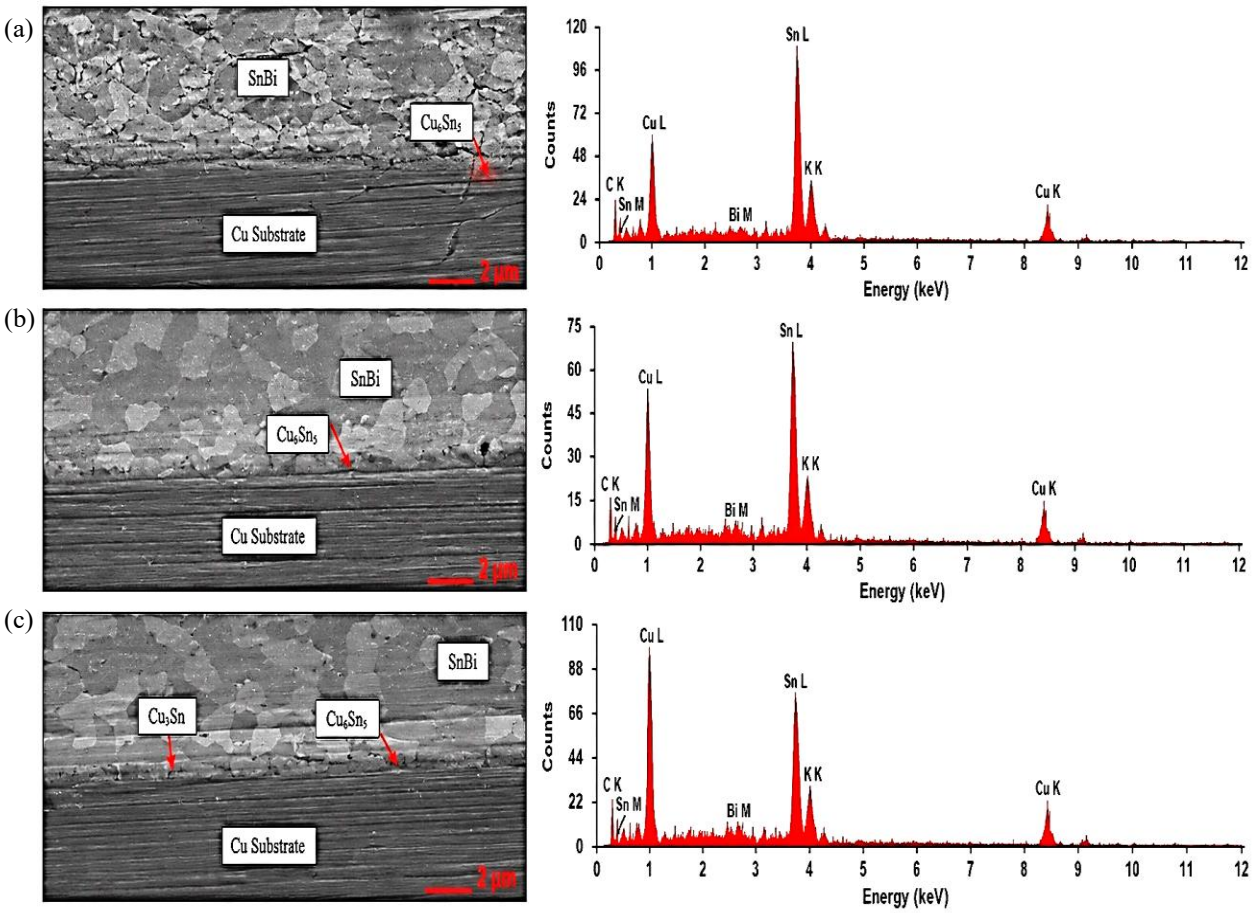

Fig. 9 EDX analysis of the IMC layer at SnBi/Cu solder joint (a) Cu_6Sn_5 layer at 170°C, (b) Cu_6Sn_5 layer at 180°C and (c) Cu_3Sn layer at 180°C.

The presence of these IMCs generally indicates good bonding between the solder and substrate, especially with a thin Cu_6Sn_5 IMC layer. At 170°C, the Cu_3Sn IMC layer was not observed, due to the low temperature and short reflow time during the reflow soldering process. Kang et al. [29] had parallel agreement where only Cu_6Sn_5 seem to be formed after reflow soldering at 170 °C for 5 minutes. Appearance of Cu_3Sn is known to be detrimental to the solder joint. In this study, at 180°C, the Cu_3Sn was detected and was alike other studies that observed the Cu_3Sn formation at 180 °C [30, 31]. Hence, the observation of this IMC is ordinary at this temperature. However, in this research, the Cu_3Sn layer formed was notably thin and the elements are unable to be identified through the EDX as seen in Fig. 9 (c).

Observing the morphologies of the IMCs at temperatures 170 and 180°C, the IMC displays relatively smooth morphologies with rounded, lumpy scallop-like curve formation. At 170 °C the average thickness of the Cu_6Sn_5 layer was 0.909µm which was thicker at 180°C with a thickness measuring 1.404µm. This observation was supported by Kang et al. [7]. In this research, it was noted that there was a more controlled IMC growth compared to the rapid increase observed at 180°C. In addition to that, a parabolic growth rate was also observed as the initial IMC growth was rapid. At 180°C, there was some detection of Cu_3Sn IMC formation near to the solder side. The diffusion theory is associated with this as the Cu is known to have higher diffusion rate and will tend to migrate into the solder side [29, 31]. Availability of high Cu content is likely to be diffused into the SnBi solder, where it reacts with Sn to form Cu_3Sn. The SEM images clearly illustrate the changes in IMC morphology at 180°C as compared to 170°C. The growth kinetics of the Cu–Sn IMCs is be determined from their measured thickness, as expressed in Eq (7).

$$X_t = \sqrt{Dt} \tag{7}$$

Alternatively, minimal Bi segregation was observed at all three reflow temperatures, suggesting that this phenomenon likely occurs at significantly higher temperatures above 180°C or after prolonged thermal aging. Investigation by Lu et al. [32] revealed that noticeable Bi segregation only emerged after approximately 10 days of aging at 180 °C. This suggest that at lower reflow temperatures below 180°C, the likelihood of Bi atoms to precipitate when Cu_6Sn_5 transform into Cu_3Sn are minimal, diminishing the Bi segregation throughout the microstructure [32,33]. This is supported by the investigation performed by Ali H et al. [27], where Bi segregation can only be observed after several days of prolonged exposure to heat. In this research, with the reflow temperature of 160, 170 and 180°C with a short reflow duration, it can be concluded that Bi segregation does not occur under these conditions.

4.0 Conclusion

The TGA and DSC confirmed the melting range of the SnBi solder is between 130 to 140 °C, confirming it being a low temperature alloy. The contact angle decreased with the increase in temperature due to the increased fluidity as the reflow temperatures increase. The spreading ratio decreased with the increase in temperature, which further supports the conclusion that elevated temperatures enhance alloy spreadability. Thinnest IMC layer was observed at 170 °C, with a thickness of 0.909 µm where the solder joint primarily consisting of Cu_6Sn_5. The Cu_3Sn was only visible at 180 °C was suggesting its formation at higher temperatures. This aligned to the thicker thickness observed. Gathering the experimental findings and analyses, the Sn58Bi can be concluded as a potential alternative for a clean low temperature solder in electronic packaging. Retardation of thick IMC layer formation and minimal formation of brittle Cu_3Sn IMC layer without jeopardizing the wettability stands out as the significant.

References

[1] F.P. Incropera, D.P. DeWitt, T.L. Bergman, A.S. Lavine, Fundamentals of Heat and Mass Transfer, 8th edn. (Wiley, Hoboken, NJ, 2017)

[2] W. Li, L. Gu, D. Li, Z.Q. Liu, Materials 17, 2848 (2024). https://doi.org/10.3390/ma17122848

[3] E. Efzan, A. Singh, Y.T. Chuen, Soldering Surf. Mount Technol. 25, 229–241 (2023). https://doi.org/10.1108/SSMT-11-2012-0026

[4] N. Ismail, W.Y. Wan Yusoff, A. Amat, N.A. Abdul Manaf, N. Ahmad, Def. Technol. 41, 134–158 (2024). https://doi.org/10.1016/j.dt.2024.05.013

[5] N.H. Mohamed Muzni, E.E. Mhd Noor, M.M.A.B. Abdullah, Nanomaterials 13, 2811 (2023). https://doi.org/10.3390/nano13202811

[6] S. Zhong, L. Zhang, M. Li, W. Long, F. Wang, Mater. Des. 215, 110439 (2022). https://doi.org/10.1016/j.matdes.2022.110439

[7] X. Wu, Z. Huo, X. Xie, P. Lim, Y. Huo, Y. Wang, X. Zhao, J. Mater. Res. Technol. 31, 3226–3237 (2024). https://doi.org/10.1016/j.jmrt.2024.07.076

[8] D.D. Tamara, B. Soegiono, B. Kurniawan, M.M. Yudi, J. Adv. Res. Mater. Sci. 18, 1–9 (2016)

[9] H. Kang, S.H. Rajendran, J.P. Jung, Metals 11, 364 (2021). https://doi.org/10.3390/met11020364

[10] P. McCluskey, R. Munamarty, M. Pecht, Microelectron. Int. 14, 20–23 (1997). https://doi.org/10.1108/13565369710800439

[11] H.-W. Miao, J.-G. Duh, Mater. Chem. Phys. 71, 255–271 (2001). https://doi.org/10.1016/S0254-0584(01)00298-X

[12] S. Zhou, C.-H. Yang, S.-K. Lin, N.A. Abdulaziz, O. Mokhtari, H. Nishikawa, Mater. Sci. Eng. A 744, 560–569 (2019). https://doi.org/10.1016/j.msea.2018.12.012

[13] Singh, R. Durairaj, IOP Conf. Ser.: Mater. Sci. Eng. 834, 012075 (2020). https://doi.org/10.1088/1757-899X/834/1/012075

[14] Torres, L. Hernandez, O. Domínguez, Mater. Sci. Appl. 3, 355–362 (2012). https://doi.org/10.4236/msa.2012.36051

[15] J.Y. Choi, D.H. Park, T.S. Oh, J. Microelectron. Packag. Soc. 19, 71–76 (2012). https://doi.org/10.6117/kmeps.2012.19.3.071

[16] G. Ren, I.J. Wilding, M.N. Collins, J. Alloys Compd. 665, 251–260 (2016). https://doi.org/10.1016/j.jallcom.2016.01.006

[17] B.S. Yim, H.J. Youn, I. Lee, J.M. Kim, J. Weld. Join. 38 (2020). https://doi.org/10.5781/JWJ.2020.38.2.4

[18] S. Griffiths, A. Wedi, G. Schmitz, Mater. Charact. 178, 111304 (2021). https://doi.org/10.1016/j.matchar.2021.111304

[19] S. He, Y. Bi, Y.A. Shen, Z. Chen, Y. Yue, C. Hu, H. Nishikawa, J. Adv. Join. Process. 6, 100118 (2022). https://doi.org/10.1016/j.jajp.2022.100118

[20] S. Jayesh, J. Elias, Mater. Today Proc. 21, 329–331 (2020). https://doi.org/10.1016/j.matpr.2019.05.455

[21] H.F. Zou, Q.K. Zhang, Z.F. Zhang, J. Mater. Res. 26, 449–454 (2011). https://doi.org/10.1557/jmr.2010.40

[22] Singh, H.L. Choo, W.H. Tan, R. Durairaj, S. Janasekaran, S.M.S. Senthil, JOM 77, 4226–4245 (2025). https://doi.org/10.1007/s11837-025-07201-9

[23] L. Jeyeselan, E.E. Mhd Noor, Materials 18, 3722 (2025). https://doi.org/10.3390/ma1816372

[24] Q. Li, N. Ma, Y. Lei, J. Lin, H. Fu, J. Gu, J. Electron. Mater. 45, 5800–5810 (2016). https://doi.org/10.1007/s11664-016-4366-z

[25] H.W. Ali, D. Drouin, N. Braidy, F. Voisard, D. Danovitch, Mater. Charact. 229, 115513 (2025). https://doi.org/10.1016/j.matchar.2025.115513

[26] J.M. Rami, C.D. Patel, C.M. Patel, M.V. Patel, Mater. Today Proc. 43, 655–659 (2021). https://doi.org/10.1016/j.matpr.2020.12.554

[27] J.R.S. Leal, R.A.V. Reyes, G.L. Gouveia, F.G. Coury, J.E. Spinelli, Metals 14, 963 (2024). https://doi.org/10.3390/met14090963

[28] O. Mokhtari, H. Nishikawa, Mater. Sci. Eng. A 651, 831–839 (2016). https://doi.org/10.1016/j.msea.2015.11.038

[29] J. Yu, J.Y. Kim, Acta Mater. 56, 5514–5523 (2008). https://doi.org/10.1016/j.actamat.2008.07.022

[30] A. Singh, S.H. Teow, R. Durairaj, A.A.Q. Saleh, J. Harbin Inst. Technol. (New Ser.) 29, 57–63 (2022). https://doi.org/10.11916/j.issn.1005-9113.2020040

[31] T.Y. Kang, Y.Y. Xiu, C.Z. Liu, L. Hui, J.J. Wang, W.P. Tong, J. Alloys Compd. 509, 1785–1789 (2011). https://doi.org/10.1016/j.jallcom.2010.10.040

[32] M. Shang, C. Li, Y. Wang, X. Chen, Y. Zhao, J. Ke, Y. Wang, H. Ma, J. Chen, J. Mater. Res. Technol. 33, 6307–6318 (2024). https://doi.org/10.1016/j.jmrt.2024.11.006

[33] H.R. Ma, C. Dong, M. Shang, M.M. Hussain, Y.P. Wang, X.G. Li, H.T. Ma, J. Chen, Mater. Charact. 171, 110830 (2021). https://doi.org/10.1016/j.matchar.2020.110830

[34] H. Li, X. Liu, L. Chen, Y. Ji, A.M. Fathy, G.A.M.M. Gaber, J. Peng, X. Zhang, A.S.A. Almalki, Z. Yang, H. Yu, X. Wang, Z. Guo, J. Rodriguez, H. Alharbi, J. Mater. Sci.: Mater. Electron. 36, 1478 (2025). https://doi.org/10.1007/s10854-025-15519-y

[35] Q.K. Zhang, H.F. Zou, Z.F. Zhang, J. Electron. Mater. 40, 2320–2328 (2011). https://doi.org/10.1007/s11664-011-1742-6